Flexural-eustatic numerical model for drowning of the Eocene perialpine carbonate ramp and implications for Alpine geodynamics

Philip A. Allen*
Department of Geology, Trinity College, Dublin 2, Ireland

Peter M. Burgess†
Department of Earth Sciences, University of Cardiff, Main Building, P.O. Box 914, Park Place, Cardiff CF10 3YE, UK

Joseph Galewsky
Department of Geology, Trinity College, Dublin 2, Ireland

Hugh D. Sinclair§
Department of Geology and Geophysics, University of Edinburgh, Grant Institute, West Mains Road, Edinburgh EH9 3JW, UK

ABSTRACT

The Paleocene–Eocene Nummulitic Limestone Formation of the Alpine periphery occupies the lowermost part of a stratigraphic trinity above a major basal unconformity. It is thought to have accumulated as a foraminiferal carbonate ramp at the distal featheredge of the underfilled north Alpine and southwest Alpine foreland basin. We present the results of a numerical model that links carbonate sedimentation at the distal featheredge of a peripheral foreland basin to the flexural subsidence of an elastic plate subjected to a distributed load with a superimposed eustatic sea-level history. Carbonate accumulation is treated as depth dependent. Model parameters are constrained by geological and geophysical observations of the Alpine orogen and its peripheral foreland basin and from literature on the ecology of benthic foraminifers.

The generic Alpine model shows that the carbonate ramp accumulates as a number of sedimentary cycles before rapid drowning, giving rise to a retrogradational stratigraphic package terminated by a surface of accelerated transgression and backstepping. Running the model with sets of parameter values appropriate to the Paleocene to middle Eocene Nummulitic Limestone in central-eastern Switzerland, and the late Eocene Nummulitic Limestone of France, results in a successful replication of the first-order characteristics of the carbonate successions in each case. The model highlights the sensitivity of the stratigraphy to variations in environmental parameters (light-extinction coefficient) and controlling tectonic parameters such as convergence rate and flexural rigidity. The results therefore also provide an interesting perspective on the likely range of geodynamical parameters, particularly equivalent elastic thickness, Te, at an early stage in Alpine orogenesis. Combined with previous estimates of Te at 25 Ma, 17 Ma, and the present day, our results appear to rule out any possible secular increase in flexural rigidity for the European plate during Tertiary time.

Keywords: Alps, carbonate ramps, foreland basins, numerical models, *Nummulites*.

INTRODUCTION

Carbonate facies occupy a number of different settings in foreland basins (Dorobek, 1995), including proximal positions on topographic highs, across the entire basin during times of reduced particulate sediment fluxes, and at the outer edge of the basin relatively distant from the contaminating influences of orogenic sediment-routing systems. The most common setting is undoubtedly the distal edge of peripheral foreland basins (proforeland basins of Johnson and Beaumont, 1995), where the carbonate successions are preserved as the lower unit of the underfilled trinity (Sinclair, 1997) (Fig. 1). The lower unit of the underfilled trinity is generally composed of shallow-marine carbonate facies. These carbonate-dominated units range from tens of meters thick, as in the early Tertiary Alpine examples from France and Switzerland, to the 1200-m-thick Miocene Darai Limestones of Papua New Guinea (Pigram et al., 1989).

The paleotopography and paleobathymetry at the distal edge of foreland basins, which strongly influence the distribution of carbonate facies, are affected by a number of local controls in addition to the first-order signature of flexural subsidence. These controls may include the effects of strike-slip deformation of the foreland, especially in the case of oblique convergence, syndepositional normal faulting due to flexural bending stresses, and reactivation of preexisting passive margin or older structures as reverse faults well ahead of the orogenic wedge. The impact of basement deformation is particularly widely reported, such as in the well-documented examples in the Late Devonian–Carboniferous Antler foreland basin of western North America (Moore, 1988; Sandberg et al., 1988; Dorobek et al., 1991) and the Mississippian to Early Permian Marathon-Ouachita foreland in the central-southeastern United States (Wuellner et al., 1986; Yang and Dorobek, 1995). Patterns of uplift and subsidence at the distal margin are superimposed by any eustatic sea-level variations, and together have a profound influence on carbonate deposition. Whereas our model results cannot account for the many local controls that influence three-dimensional strati-

*E-mail: paallen@tcd.ie.
†E-mail: burgesspm@cardiff.ac.uk.
§E-mail: hugh.sinclair@glg.ed.ac.uk.

GSA Bulletin; August 2001; v. 113; no. 8; p. 1052–1066; 12 figures; 4 tables.

graphic geometries in distal foreland basins, they provide a set of one-dimensional benchmarks for the stratigraphic expression of carbonate accumulation under a simple combined flexural-eustatic mechanism.

The characteristic depositional environment for carbonates in the early Tertiary peripheral Alpine foreland basin of France and Switzerland is thought to be the distal featheredge of the basin above a variably developed flexural forebulge unconformity (Allen et al., 1991; Crampton and Allen, 1995). The demise of these carbonate ramps is marked by a deepening of sedimentary facies, reflecting a drowning of the carbonate depozone. The carbonate succession consists of a number of primarily shallowing-upward cycles. The assemblage of component facies within these cycles suggests that they are arranged in a variety of retrogradational (backstepping), aggradational, and progradational stacking patterns before final drowning. Our aim is to explain the thickness, cycles, stacking patterns, and drowning of the Eocene carbonate ramps in relation to a set of geodynamic, paleoecological, and sedimentological parameters. Geodynamic parameters can rarely be well defined in geological case studies (exceptions are Yang and Dorobek, 1995; Sinclair, 1997). However, the evolution of the Alpine orogenic wedge and peripheral foreland basin development in France and Switzerland are now known well enough to allow a successful test of a numerical model for carbonate drowning (Galewsky, 1998). We conclude that the carbonate ramps around the outer edge of the Alpine foreland basin in Switzerland and France developed at the distal feather edge of a flexural foredeep under a precise combination of geodynamic, eustatic, ecologic, and sedimentological conditions, although we cannot rule out the possibility of partial deposition in bulge-top positions (sensu DeCelles and Giles, 1996). Our results therefore confirm the perialpine carbonate ramps as distal foredeep deposits and in addition allow a refinement of ideas on the early Tertiary development of the orogen-basin system. The links established between stratigraphic architecture and forcing mechanisms will be of use in investigating analogous deposits in other foreland basins worldwide.

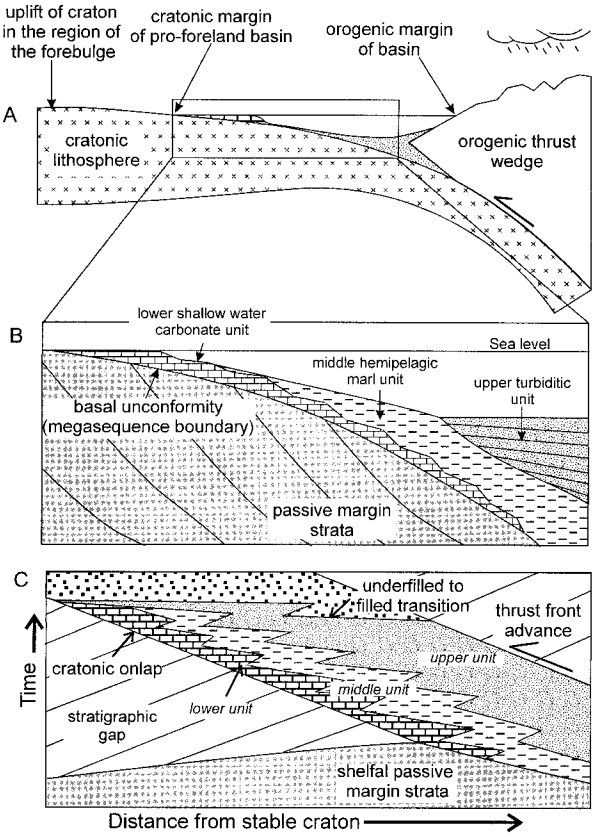

Figure 1. General scheme of the underfilled trinity of foreland basins, adapted from Sinclair (1997). (A) Location of carbonates at distal margin of peripheral foreland basin. (B) Underfilled trinity of basal shallow-water limestones, hemipelagic marls, and turbidites derived from the orogen (s.l.—sea level). (C) Chronostratigraphic diagram showing diachronous migration of facies belts over foreland plate.

OVERVIEW OF THE EARLY TERTIARY PERIALPINE CARBONATE RAMPS IN FRANCE AND SWITZERLAND

During the early underfilled stage of the Alpine peripheral foreland basin a carbonate ramp developed around the distal edge of the flexural foredeep (Fig. 2) (Allen et al., 1991; Sinclair, 1997), as in other examples in analogous basin settings (e.g., Jacobi, 1981; Tankard, 1986; Pigram et al., 1989; Dorobek, 1995). The carbonate ramp, known as the Nummulitic Limestone, is well exposed and has been intensively studied in both Switzerland and southeastern France (Bodelle, 1971; Campredon, 1977; Lateltin and Muller, 1987; Herb, 1988; Crampton, 1992; Crampton and Allen, 1995; Sinclair et al., 1998). It forms the basal part of the underfilled trinity developed above the basal Tertiary unconformity (Fig. 3) (Boussac, 1912; Sinclair, 1997). This basal unconformity has been interpreted as a flexural forebulge unconformity in eastern Switzerland (Crampton and Allen, 1995); the underfilled trinity is interpreted as a deepening-upward succession from distal carbonate ramp to pelagic marls to orogen-derived siliciclastics. These three facies associations occur diachronously across the foreland basin (Fig. 1), younging to the north-northwest in Switzerland (Boussac, 1912; Schumacher, 1948; Herb, 1988) and to the west and southwest in France (Martini, 1968; Pairis, 1988). This supports the view that the trinity represents coeval facies belts in an asymmetrical foreland basin flexed downward by an Alpine load system, which migrated onto the European craton during early Tertiary time.

Structural Setting

The Nummulitic Limestone and other units in the underfilled trinity are found in a number of different settings around the Alpine arc (Fig. 2). In Switzerland the Nummulitic Limestone is found in the nappes of the Helvetic Alps and in the deformed (but not detached) sedimentary cover of Hercynian crystalline basement massifs such as the Aar (Trümpy, 1980; Pfiffner, 1986; Herb, 1988; Allen et al., 1991; Crampton, 1992). Similar sediments are found in large

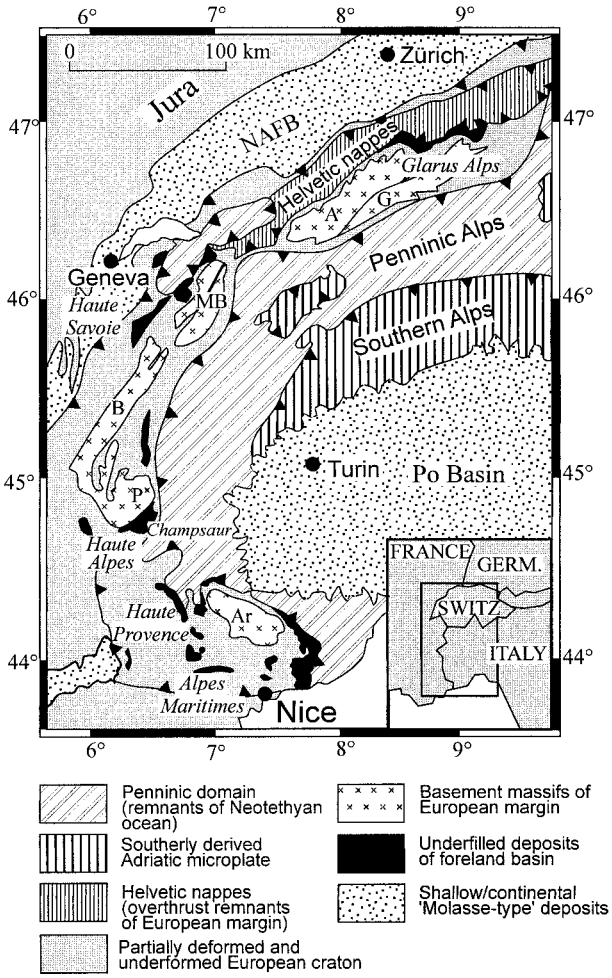

Figure 2. Occurrence of underfilled foreland basin deposits (including the Nummulitic Limestone) around the Alpine arc in France and Switzerland, showing main tectonic units and locations discussed in text. A—Aar, G—Gotthard, MB—Mont Blanc, B—Belledonne, P—Pelvoux.

footwall synclines in the Haute Savoie area near the France-Switzerland border (Lateltin, 1988; Butler, 1989; Guellec et al., 1990; Mugnier et al., 1990). Farther to the south, they are found in thrust sheets around the eastern margin of the Pelvoux Massif (Barbier, 1956; Deharveng et al., 1987) and in its slightly deformed cover in the Champsaur district of les Hautes Alpes (Waibel, 1990; Gupta, 1994). Additional exposures are found in Haute Provence and les Alpes Maritimes in synclines on top of Alpine southwest-directed thin-skinned structures (Lemoine, 1972; Elliott et al., 1985; Pairis, 1988; Lickorish and Ford, 1998) and east-west–oriented folds related to the Pyrenean-Provençal phase of deformation (Goguel, 1936; Lemoine, 1972; Siddans, 1979).

Underlying Succession

A pre-Nummulitic Limestone succession is preserved in structurally controlled topographic lows beneath the Nummulitic Limestone locally, especially in the French sector of the basin (Haute Savoie, Champsaur district of les Hautes Alpes, Alpes Maritimes). These pre- or Infranummulitic Limestone sediments record subaerial, shallow-marine, littoral, lagoonal, and estuarine environments developed prior to Nummulitic Limestone transgression. The precise structural controls vary from one area to another. In Haute Savoie (Chaplet, 1989; Lateltin and Müller, 1987), the structural paleotopography has been linked to the early stages of extension in the western European rift system (Pairis and Pairis, 1975; Ziegler, 1988). Normal faults along the basin margins have offsets of tens of meters and generated significant paleorelief (Lateltin and Müller, 1987; Sayer, 1995). Much of this relief was reduced by the accumulation of alluvial and lagoonal sediments in topographic lows prior to transgression and establishment of the Nummulitic Limestone carbonate ramp (Sinclair et al., 1998). In the Champsaur area, the structures are reverse faults (Ford, 1996; Gupta, 1997) that have been interpreted in terms of inversion of passive margin half graben together with crystalline basement, such as the Pelvoux Massif, in response to Alpine compression (Gupta and Allen, 2000). In the Alpes Maritimes, the structures are associated with east-west folds and faults linked to the Paleocene–early Eocene Pyrenean-Provençal orogenic phase (Debrand-Passard, 1984). In these localities Infranummulitic Limestone sediments pass via a ravinement surface into open-marine carbonate facies dominated by large foraminifers.

In the Helvetic nappes of central-western Switzerland, terrestrial sediments, locally pisolitic iron-rich sandstones and breccias (Zwahlen, 1986), fill cracks, fissures, and irregularities in the Mesozoic substrate. These terrestrial sediments, known as sidérolithique, are thought to have formed on an uplifted, karstified land surface during Paleocene–Eocene time (Wieland, 1976; Trümpy, 1980; Wiedmann, 1984). Where the Infranummulitic Limestone rocks are absent, as in the parautochthon of the Aar Massif in eastern Switzerland, eroded and slightly tilted Mesozoic rocks are abruptly overlain by transgressive marine greensands followed by foraminiferal limestones (Herb, 1988; Allen et al., 1991; Crampton, 1992).

Facies and Facies Cycles

The Nummulitic Limestone contains a range of facies, which together suggest deposition on a carbonate ramp, similar to those interpreted from the Tertiary of Egypt and Oman (Aigner, 1983; Racey, 1990). The inner ramp comprised bioclastic shoals dominated by either peloids or nummulitids (Alpes Maritimes and Switzerland) or calcareous red algae (Haute Savoie). Middle ramp sediments consist of foraminiferal and foraminiferal-algal wackestones and packstones with robust forms such as *Nummulites* and *Amphistegina* found in the uppermost strata of middle ramp facies, and slender, flat *Discocyclina* and *Operculina* in the lowermost strata of middle ramp facies. The outer ramp consisted of mud-

stones, marls, and siltstones, with abundant nektonic bivalves (Crampton, 1992; Sinclair et al., 1998).

The Nummulitic Limestones are in general organized in distinct shallowing-upward cycles, separated by surfaces of rapid deepening; details within cycles, their frequency, number, and total thickness vary from one locality to another (Figs. 4 and 5) (Table 1). In broad terms, however, the late Paleocene to mid-Eocene cycles preserved in Switzerland are thin (<10 m), of long duration (>1 m.y.) and few in number (<3), whereas the late Eocene examples preserved in France are thin to very thin (few to 10 m), short in duration (<500 k.y.) and large in number (<10). The total thickness of the Nummulitic Limestone can reach 70 m, as in the Platé area of Haute Savoie (Pairis and Pairis, 1975), due to synsedimentary faulting, and 80 m in the Champsaur district of les Hautes Alpes (Gupta, 1994), where incised valley fills are preserved (Gupta, 1997), but total thicknesses are generally <40 m. Variability is also particularly marked in Haute Savoie, where inherited structural heterogeneity continued to influence Nummulitic Limestone facies and cycle thicknesses (Lateltin and Müller, 1987; Villars et al., 1988). Although paleorelief was reduced by deposition of pre-Nummulitic Limestone sediments, enough structural paleotopography was present to cause the nondeposition or erosion of as many as three Nummulitic Limestone cycles over structural highs. In most localities throughout the France-Switzerland area, the uppermost cycle is abruptly terminated by a surface of major backstepping, representing the final drowning of the carbonate ramp at that particular locality.

Although the long-term trend from subaerial emergence of the foreland, inundation, and ramp drowning is retrogradational, sets of cycles are commonly stacked in progradational and aggradational patterns. For example, in the Thones syncline, Haute Savoie at Chinaillon, eight aggradational to progradational cycles total 38 m in thickness (Sinclair et al., 1998); middle to outer ramp facies dominate lower cycles and inner ramp facies dominate upper cycles, suggesting that the overall stacking pattern below the ramp drowning surface is progradational rather than retrogradational. Retrogradational carbonate ramps are cited as typical of a range of distal foreland basins, including the Middle Ordovician of Virginia and Tennessee (Read, 1980; Ruppel and Walker, 1984), the Mississippian Lodgepole Formation of Montana (Elrick and Read, 1991), the Mississippian Fayetteville Limestone of

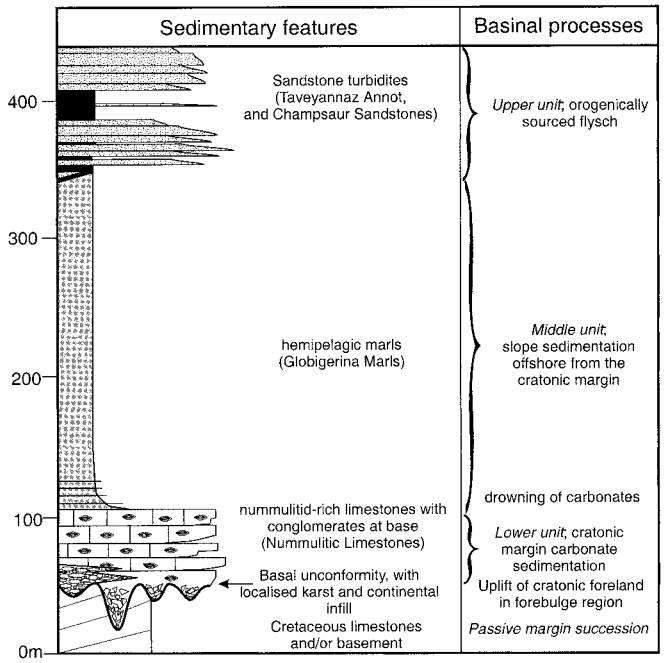

Figure 3. The stratigraphy of the Nummulitic Limestone at the megasequence boundary between the underlying passive margin and the overlying foreland basin fill.

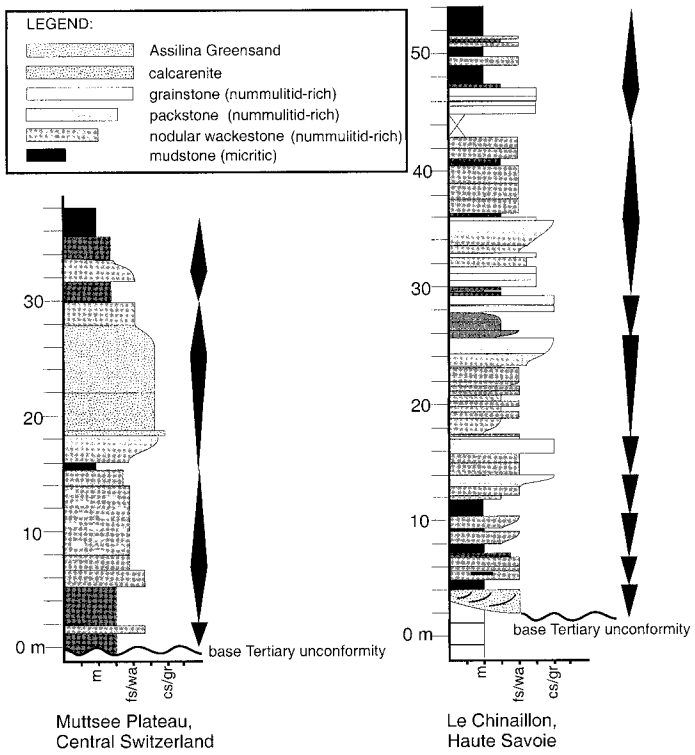

Figure 4. Sedimentological logs of the Nummulitic Limestone in central Switzerland (Muttsee plateau, Glarus) (Crampton, 1992) and in Haute Savoie, France (Le Chinaillon) (Sayer, 1995). The sections in France are generally thicker and composed of a larger number of high-frequency cycles. Fs/wa—fine sandstone or wackestone, cs/gr—coarse sandstone or grainstone.

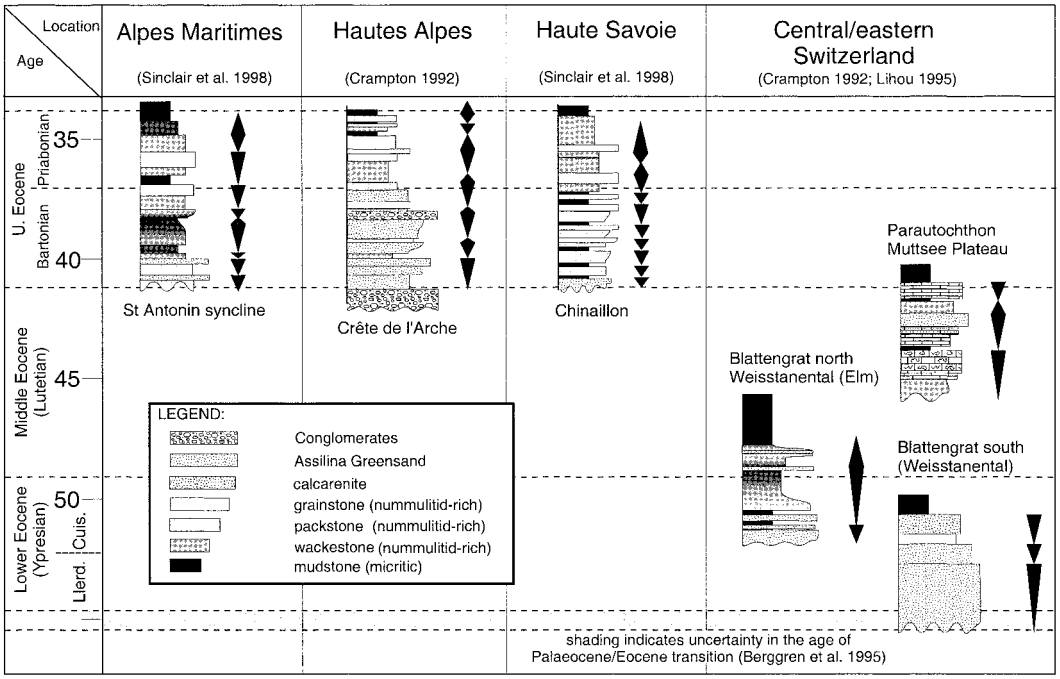

Figure 5. Schematic illustration of facies cycles around the Alpine arc from southeastern France to eastern Switzerland in their chronostratigraphic position.

TABLE 1. CYCLES IN THE NUMMULITIC LIMESTONE IN SWITZERLAND AND FRANCE USED TO CONSTRAIN MODEL PARAMETERS

Stratigraphic or tectonic unit	Biostratigraphic age	Cycle duration and number; stratigraphic thickness	References
Blattengrat unit, eastern Switzerland, south Helvetic zone; Einseidler Limestone, Helvetics, Sihltal	Fliegenspitzschichten and basal sandstone of Batöni Formation are Paleocene; Batöni Sandstone Member is mid-late Cuisian; Nummulitic Limestone Member is Cuisian to early Lutetian. Fleckenmergel (Lutetian–Priabonian) marks ramp drowning	Batöni Sandstone 30 m; Nummulitic Limestone 20 m in northwest, 50 m in south and southeast; average cycle duration 3 m.y. based on Palaeocene-Lutetian interval; 4 cycles in Ilerdian to Cuisian (6.5 m.y.), giving cycle duration of ~1.5 m.y.	Blattengrat: Bisig (1957), Rüeffli (1959), Wegmann (1961), Lihou (1995), Lihou and Allen (1996). Einseidler Limestone: Bisig (1957), Wegmann (1961), Stacher (1980).
Aar Massif parautochthon, central-eastern Switzerland, Glarus and Graübunden, Helvetic zone	Bürgen Formation is mid-Lutetian. Pecten beds represent ramp drowning in late Lutetian	2 to 3 cycles in any locality; e.g., Kistenpass, each ~10 m thick; 20 m preserved beneath major backstep surface; duration <2 m.y.	Heim (1909), Leupold (1966), Herb (1988), Crampton (1992), Crampton and Allen (1995).
Helvetic thrust sheets; e.g., Sanetsch, Valais	Hohgant Formation is Priabonian	3 cycles, each 5–10 m thick; average duration <1 m.y.	Breitschmid (1978), Steffen (1981), Zwahlen (1986).
Haute Savoie, France, Thones syncline	Le Chinaillon locality, Nummulitic Limestone is Priabonian	Up to 8 cycles, each 1 to 10 m thick, duration <400 k.y.; 33 m below major backstep surface, 20 m above	Sinclair et al. (1998)
Alpes Maritimes, France, northern synclines (Annot, Argens, Agneres)	Nummulitic Limestone Formation is Priabonian	4–6 cycles in northern synclines; 6 cycles at Ivoire (32 m below major backstep surface); 8 cycles at St. Antonin (42 m below major backstep surface)	Sinclair et al. (1998)
Les Haute Alpes, Champsaur district; e.g., at Crete de l'Arche, parautochthon of Pelvoux Massif	Nummulitic Limestone Formation is Priabonian	7 wave cut platforms and risers, each ~10 m thick; duration of <500 k.y.; Nummulitic Limestone <80 m thick	Gupta (1994), Gupta and Allen (1999)

Arkansas (Handford, 1993), and the Upper Pennsylvanian to Lower Permian Val Verde basin and Marathon region of western Texas (Ross and Ross, 1985; Yang and Dorobek, 1995). The precise stacking pattern of cycles most likely reflects a complex local interplay of carbonate production rates and creation of accommodation space, and is not reproducible in the generalized numerical model as currently formulated (see following).

PALEOECOLOGY OF THE NUMMULITE BANKS

Numerical models of drowning have been developed for coral reefs subjected to eustatic sea-level rise (e.g., Bosscher and Schlager, 1992). The Nummulitic Limestone of the perialpine early Tertiary is composed primarily of the skeletons of large benthic foraminifers. It is therefore necessary to know something about the paleoecology and paleoenvironments of these benthic organisms.

It is believed that larger Eocene foramini-

fers were equipped with symbiotic algae, as in modern relatives such as *Heterostegina*. For symbionts to function, sufficient light would be required. Consequently, foraminiferal hosts must have lived in the euphotic zone at depths of <150 m (Racey, 1990), but probably >5 m, because too much light retards growth (Röttger, 1976; Hallock, 1985). The ideal illumination depth range for symbionts varies with the turbidity of the water. However, the modern *Heterostegina* functions best under 300 lux in the laboratory (Röttger, 1976), and occurs in depths of 1−88 m in modern seas (Reiss and Hottinger, 1984).

The need to make efficient use of light levels may explain variations in shape, i.e., thin flat forms in deeper water and more inflated, globular forms in shallower water: modern forms such as *Operculina* show this (Reiss and Hottinger, 1984). A large size has been suggested as advantageous for existence at low nutrient levels (Hallock, 1985). If this is the case, the abundance of the large *Nummulitids* and *Discocyclinids* in the Swiss Nummulitic Limestone may indicate generally low nutrient levels.

Brasier (1980) proposed that the ratios of planktic, agglutinated, and benthic forms reflect water depths. Planktic forms are only significant at water depths >80−100 m, and are extremely rare in water depths shallower than 40 m.

These considerations allow the component facies of the Nummulitic Limestone to be interpreted in terms of carbonate ramp subenvironments. Details of the high-frequency stratigraphy of the Nummulitic Limestone around the Alpine arc are summarized in Table 1 and depicted in Figures 4 and 5. Sedimentological details can be found in the references cited therein.

TABLE 2. ESTIMATES OF EQUIVALENT ELASTIC THICKNESS FOR THE ALPINE FORELAND

Location	Te (km)	Authors
Based on gravity data		
Western Switzerland	20	Karner and Watts (1983)
Eastern Switzerland	50	Karner and Watts (1983)
Alps and Molasse basin	15	Lyon-Caen and Molnar (1989)
Western Alps	30–39	Macario et al. (1995)
Eastern Alps	33–40	Macario et al. (1995)
Whole Alps	27	Macario et al. (1995)
Western Alps	5–15	Stewart and Watts (1997)
Western Swiss Alps	25	Burkhard and Sommaruga (1998)
French Alps and eastern Switzerland	~30	Stewart and Watts (1997)
Alps and Molasse basin	50	Royden (1993)
Based on stratigraphic studies		
Central Switzerland at 17 Ma	10±5	Sinclair et al. (1991)
Central Switzerland at 25 Ma	10–15	Schlunegger et al. (1997)
Alpine arc, Switzerland, and southeast France, Eocene	<17	Sinclair (1996)
Based on thermokinematic modeling		
North Alpine foreland (broken plate)	25	Okaya et al. (1996b)
North Alpine foreland (continuous plate)	40	Okaya et al. (1996b)

TABLE 3. KINEMATIC DATA FROM THE ALPINE WEDGE

Location of transect	Time interval	Pinch-out migration and thrust advance rate (mm yr^{-1})	References
Flysch phase			
Switzerland	Latest Maastrichtian to mid-Oligocene	6–12	Sinclair and Allen (1992)
Western Switzerland	Eocene to mid-Oligocene	10–14	Sinclair and Allen (1992)
Western Switzerland	Oligocene (40–30 Ma)	10–20	Burkhard and Sommaruga (1998)
Switzerland	Eocene	8–13	Sinclair (1997)
France	Eocene	5–8	Sinclair (1997)
Eastern Switzerland	Eocene to mid-Oligocene	3–4	Pfiffner (1986)
Alpine region	Mid-Cretaceous to early Eocene	~10	Sinclair and Allen (1992)
Eastern Switzerland Geotraverse	Eocene (50–40 Ma)	15	Schmid et al. (1996)
Alpine region	Eocene (51–38 Ma)	12	Dewey et al. (1989)
Molasse phase			
Western Switzerland	Oligocene (30–22 Ma)	5	Burkhard and Sommaruga (1998)
Switzerland	Late Oligocene to Miocene	1–4	Sinclair and Allen (1992)
Central-eastern Switzerland	Miocene	2–4	Sinclair et al. (1991)
Western Switzerland	Oligocene	7–9	Homewood et al. (1986)
Western Switzerland	Miocene	2	Homewood et al. (1986)

MODEL DESCRIPTION

Numerical models of carbonate stratigraphy are based on a depth-dependent carbonate production function that is linked to known trends of light attenuation with depth in the ocean (Bice, 1991; Bosscher and Schlager, 1992). Shallowing-upward cycles up to a few tens of meters in thickness have been modeled numerically by a simple superimposition of this depth-dependent carbonate production function and a sinusoidal eustatic curve (Goldhammer et al., 1987; Spencer and Demicco, 1989; Watney et al., 1991). The one-dimensional numerical model used in this study links carbonate sedimentation with flexural subsidence of an elastic plate, initially developed by Galewsky (1998) to model coral platforms offshore Papua New Guinea. There are two considerations when using this model to understand the Alpine Nummulitic Limestone. First, the Alpine carbonate accumulations represent nummulite banks rather than coral buildups; second, there is a correlation between the maximum rate of platform growth and observational interval (Sadler, 1981; Schlager, 1999). Consequently, the value of the maximum growth rate of Holocene reefs needs to be decreased to represent the Eocene Alpine examples.

In contrast to the carbonate sediments of coral platforms, the carbonate sediments produced within a nummulite bank are potentially subject to significant transport or dissolution (Hallock, 1981). Thus, the relationship between carbonate production rates and sediment accumulation rates is potentially complex. The coral-growth algorithm of Bosscher and Schlager (1992) used by Galewsky (1998) scales a maximum upward coral growth rate with the depth-dependent extinction of photosynthetically active light. In most Holocene coral reefs, this maximum upward growth rate is ~10 mm yr^{-1} (see Schlager, 1999, for a compilation of Caribbean and Indo-Pacific examples). The growth of large foraminifers is, like that of corals, dependent on the amount of light available for photosynthesis (e.g., Hallock et al., 1986). However, the accumulation

rates for banks of large foraminifers are thought to be substantially less than the maximum growth rate of corals, or ~0.01–0.9 mm yr^{-1} (Hallock, 1981), i.e., 1−2 orders of magnitude smaller than the Holocene coral growth rates. We take a maximum foraminiferal growth rate of 0.02 mm yr^{-1}, toward the lower end of this range, in recognition of the observational interval of the Eocene examples (Schlager, 1999). Although this value is to some extent arbitrary, it is consistent with the carbonate production functions of Gildner and Cisne (1990) and Demicco (1998). To obtain the accumulation rate as a function of depth, we scale the accumulation rate of the nummulite banks by the depth-dependent photosynthesis function of Bosscher and Schlager (1992).

Subsidence is modeled as the flexural deformation of an elastic plate subjected to a distributed load (Jordan, 1981). The load is modeled as a simple taper composed of crustal density rocks (average density of 2500 kg m^{-3}) infilling the deflection, with a maximum surface elevation at the rear of the wedge. The flexural effects of sediment accumulation and of eustatic sea-level variations are not considered. Eustatic sea-level variations are modeled as a sinusoidal curve. Kominz et al. (1998) showed that the eustatic variation in the Paleogene was 0.5−3 m.y. in period and a few tens of meters in maximum amplitude. During each 50 k.y. time step, the position of the load advances toward the foreland at a predefined convergence rate. The tectonic subsidence due to the encroaching load is calculated using the equation for elastic plate flexure, and the new depth of the plate relative to eustatic sea level during that time step is calculated. The upward growth of the carbonate ramp is calculated, based on the depth of the ramp during that time step, and new growth is added to the ramp. If the growth of the ramp is limited by a lack of accommodation space, the model allows the ramp to grow to sea level, and the excess carbonate that would have been produced is not considered further. In reality, however, the excess carbonate would be transported basinward with the net effect of ramp progradation. Thus, even though the tectonic subsidence in a foreland basin supports an overall pattern of carbonate ramp retrogradation (Galewsky, 1998), periods of very low sea-level variation or of vigorous carbonate production may lead to progradation of the carbonate ramp into the foreland basin, as seen from our field data.

The model space is 100 km long, divided into 100 m cells. The height of the plate with its developing carbonate ramp is updated after every 50 k.y. time step. A point is reached, under certain combinations of parameters, when the upward growth rate of the ramp cannot compensate for the accommodation space generated during that time step, at which point the ramp is drowned. The output of the model gives the total time elapsed before drowning,

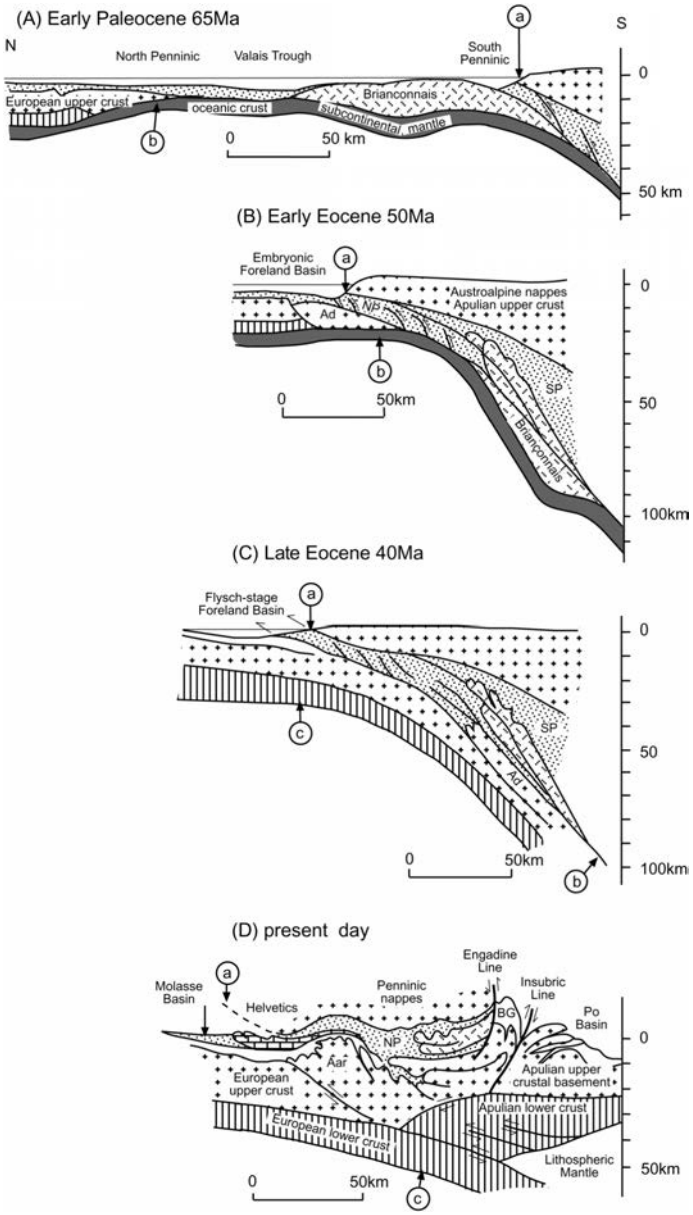

Figure 6. Restorations of crustal-scale geometry of the Alpine orogen in the early Paleocene (A), early Eocene (B), and late Eocene (C), together with the present-day cross section (D). The present-day cross section is derived from seismic reflection and refraction profiling along a north-south transect close to the border of Switzerland and Austria (Schmid et al., 1996). a—The northernmost position of the Apulian upper crust, represented by the Austroalpine nappes. b—The southernmost European crust situated north of the Valais Trough (Trümpy, 1980) at 65 Ma becomes initially subducted at 50 Ma (Stäuble and Pfiffner, 1991; Froitzheim et al., 1996; Schmid et al., 1996), and metamorphosed to eclogite facies (Adula nappe) by 40 Ma at depths of 50–90 km. c—Reference point in the European lower crust. Ad—Adula crust, NP—North Penninic metasediments, SP—South Penninic metasediments (Bündnerschiefer); BG—Bergell Granite.

the total thickness of carbonate deposited, cycle thicknesses, and water depth of deposition. The latter three ouputs can be directly compared with preserved ramp deposits. Limitations in biostratigraphic control generally permit only a coarse test of the model with observed durations of carbonate accumulation. Water depths, sea level, depth to basement, and depth to the top of the carbonate bank are tracked through model time and presented graphically here.

The one-dimensional model outputs are directly comparable with field sections or borehole records. Because the distal foreland basin carbonate facies belt migrates diachronously across the foreland ahead of the orogenic load, the one-dimensional sections apply to all positions in the foreland basin, except those that were inboard of the first node at the very onset of flexure. Such localities are unlikely to have preserved distal carbonate facies and therefore can be neglected from this study.

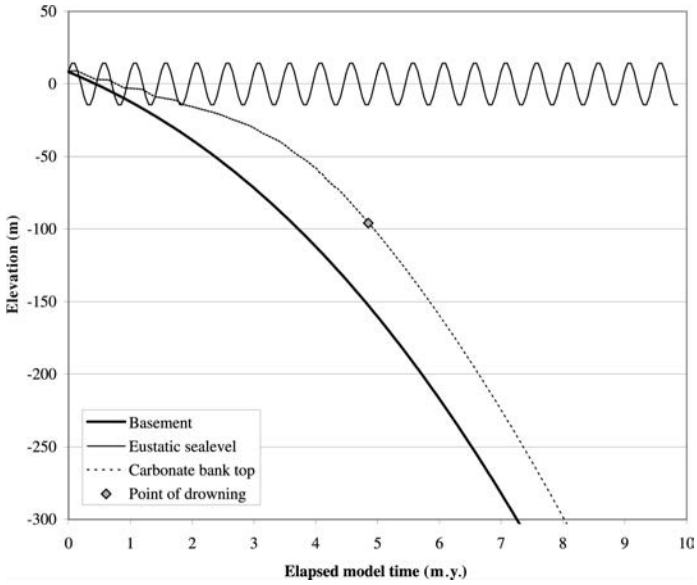

Figure 7. Generic Alpine model run using the set of parameter values shown in Table 4. See text for discussion.

CONSTRAINTS ON MODEL PARAMETERS FROM THE ALPINE CASE STUDY

Amplitude and Frequency of the Eustatic Signal

The preserved thicknesses of the cycles in the Nummulitic Limestone cannot be directly used to estimate the amplitude of the presumed eustatic forcing mechanism for relative sea-level change. It is noteworthy that only a fraction of the possible paleobathymetric range of a nummulite limestone ramp is preserved in the facies that comprise individual cycles. However, using the water depth estimates based on paleoecological studies, there must have been several tens of meters of change in water depth through individual cycles in the late Paleocene to mid Eocene examples in central-eastern Switzerland, but somewhat smaller values in the Priabonian examples in France and western Switzerland.

The frequency of eustatic change is extremely difficult to assess from field data (Table 1). Relative dating of the Nummulitic Limestone in Haute Savoie, Alpes Maritimes, and les Haute Alpes based on the foraminiferal assemblage (Bodelle, 1971; Mougin-Grosso and Pairis, 1973; Campredon, 1977), the age of the underlying Infranummulitic Limestone interval based on the occurrence of the gastropod *Cerithium diaboli* (Pairis, 1988) and vertebrate remains (Weidmann et al., 1991), and the faunal assemblage of the overlying Globigerina marls, merely allows the Nummulitic Limestone to be assigned to the Priabonian—a time window of more than 3 m.y. (Berggren et al., 1995). Using these age limitations, the maximum duration of individual stratigraphic cycles is likely to be in the range of 400−500 k.y. (Table 1).

As many as seven wave-cut platforms and six risers have been identified in the Priabonian Nummulitic Limestone at Crête de l'Arche in the Champsaur district (Gupta and Allen, 1999). Magnitudes of sea-level change of as much as 30 m can be estimated from paleocliff heights.

The Nummulitic Limestone and associated formations in eastern-central Switzerland span a larger interval, from Paleocene to Lutetian time (Table 1). Few cycles are preserved at any locality; e.g., only 2−3 cycles are preserved in the Lutetian Bürgen Formation in the Kistenpass region of the Aar parautochthon in Canton Glarus (Herb, 1988; Allen et al., 1991; Crampton, 1992). Cycles in Paleocene to middle Eocene strata in east-central Switzerland therefore appear to have had longer durations (>1 m.y.) than their counterparts in the upper Eocene strata of France.

These estimates from field observations fully accord with the independent estimates of eustatic frequencies and amplitudes calculated by Kominz et al. (1998) for Paleogene time.

Flexural Rigidity of the European Plate

The flexural rigidity of the European plate during Alpine orogenesis has been estimated by a number of different methods (Table 2). (1) Gravity (Bouguer anomaly) data have been matched with the modeled gravity field calculated for given values of flexural rigidity (Karner and Watts, 1983; Lyon-Caen and Molnar, 1989; Stewart and Watts, 1997). (2) Inverse modeling has used the coherence between surface topography and the gravity field (Macario et al., 1995). (3) The deflections of the present-day basement and the gravity field have been used as a constraint in a dynamical model of flexure of a broken plate (Royden, 1993). (4) Present-day geometry derived from seismic experiments (Burkhard and Sommaruga, 1998) and retrodeformed basin stratigraphy at certain time slices (17 Ma, Sinclair et al., 1991; 25 Ma, Schlunegger et al., 1997a) have been used to reconstruct cross-sectional basin geometry and matched with predicted profiles for different values of flexural rigidity. (5) The plan view curvature (and paleocurvature derived from points of onlap of the Nummulitic Limestone on the European craton) of the Alpine arc has been correlated with flexural rigidity (Sinclair, 1996; discussion by Zweigel and Zweigel, 1998). (6) Thermokinematic modeling allows the calculation of strength envelopes across the orogen, and thereby estimates of flexural rigidity (Okaya et al., 1996a, 1996b).

There is considerable evidence that the flexural rigidity (expressed as equivalent elastic thickness, Te) of the European plate in western Switzerland is currently very weak (~10 km). This weak zone coincides spatially with the

TABLE 4. SUMMARY OF INPUT PARAMETERS, AND MODEL OUTPUT AND FIELD-BASED ESTIMATES

Input parameter	Generic Alpine case (Sensitivity tests)	French late Eocene	Swiss early to middle Eocene
Flexural rigidity expressed as elastic thickness	20 km (15, 25 km)	15 km	25 km
Tectonic advance rate in Eocene	8 mm yr^{-1} (4, 8, 12 mm yr^{-1})	8 mm yr^{-1}	12 mm yr^{-1}
Maximum carbonate productivity	20 m $m.y.^{-1}$	20 m $m.y.^{-1}$	20 m $m.y.^{-1}$
Light-extinction coefficient	0.05 m^{-1} (0.025, 0.075 m^{-1})	0.05 m^{-1}	0.05 m^{-1}
Amplitude (half excursion) of eustatic variation	15 m	10 m	20 m
Period of eustatic variation	500 k.y.	400 k.y.	1 m.y.
Field-based estimates			
Duration of carbonate deposition		3 m.y.	6.5 m.y.
Thickness of carbonate deposit		<40 m	20–30 m
Number of cycles		<9	2–3
Model output	Figure 7	Figure 12	Figure 11
Duration of carbonate deposition	5 m.y.	2.7 m.y.	2.7 m.y.
Thickness of carbonate deposit	60 m	36 m	25 m
Number of cycles	10	8	3

region of heating associated with the western European rift system. Because this rifting is late Eocene, especially early Oligocene, in age, it is questionable whether it affected the backstepping and drowning of the Nummulitic Limestone. In addition, Alpine shortening has now compressed the zone between the outcrops of Nummulitic Limestone and the western European rift system. A palinspastic restoration to the Eocene would place the future site of the Rhine Graben more than 200 km from the stratigraphic pinch out of the Nummulitic Limestone, and perhaps twice that from the edge of the subducted European plate.

Away from the weak zone in western Switzerland, estimates of Te vary widely according to the techniques used (Table 2). A number of estimates based on a variety of methods consistently give elastic thicknesses to ~25 km. We therefore use values of elastic thickness between 15 km and 25 km in the generic model.

Kinematics of the Alpine Wedge

The advance rate of the thrust front in Switzerland during the Tertiary was documented by Homewood et al. (1986), Sinclair et al. (1991), Sinclair and Allen (1992), and Sinclair (1997) on the basis of bracketing of proximal basin margin fault activity by the ages of the youngest stratigraphy cut by the fault and of the oldest stratigraphy draping the fault. Sinclair and Allen (1992) proposed a fast-moving, low-angled taper in Eocene time, corresponding to the so-called flysch stage, compared to a slow-moving, more steeply tapered orogen in the so-called molasse stage. They identified an increase in the exhumation rate of the orogenic wedge at the time of slowing of the frontal advance rate.

There is a decoupling of the rate at which a wedge advances over the stratigraphy of the foreland plate and the rate of influx of mass into the orogenic zone driven by plate convergence (Hardy et al., 1998). Consequently, the frontal advance rate cannot be used directly as a surrogate for the migration of a spatially variable load over the foreland plate. Although there have been attempts to reconstruct the structural, denudational, and stratigraphic evolution of the orogen and foreland basin during the Oligocene–Miocene molasse phase (Schlunegger et al., 1997a, 1997b, 1998), a similar approach for the Eocene phase of the basin is more difficult because of the uncertainties in structural restoration and paleowater depths. The time-averaged rates are summarized from various sources in Table 3.

The rate of convergence between the European plate and the southern indenting plate (or microplate) can be estimated from relative plate-motion studies (Dewey et al., 1989) and from retrodeformation studies (Schmid et al., 1996; Burkhard and Sommaruga, 1998) (Fig. 6). The overall time-averaged convergence rates from 65 Ma to the present for the two methods are strikingly similar (Table 1; Schmid et al., 1996, p. 1054) (7.2 mm yr^{-1} vs. 7.9 mm yr^{-1}, respectively). There are some interesting differences between the two approaches over smaller time periods, but the general picture is coherent (Table 3). Both studies indicate a slowing of the convergence rate into Oligocene time, and especially through Miocene time. This trend strongly supports the tectono-stratigraphic techniques of Homewood et al. (1986), Pfiffner (1986), Allen et al. (1991), Sinclair and Allen (1992), and Sinclair (1997). We take a range of 8–12 mm yr^{-1} for the Eocene in our ramp-drowning model. Sinclair (1997) also compiled rates of distal pinch-out migration of the underfilled basin, and obtained a rate of 8–13 mm yr^{-1}. The similarity of this range to the tectonic rates given here is suggestive of an orogen and basin that were migrating across the European foreland in a steady-state fashion.

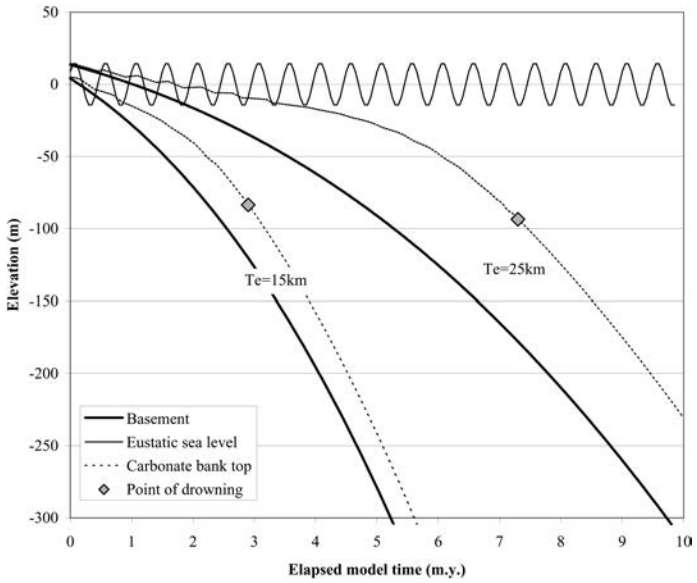

Figure 8. Model results using equivalent elastic thicknesses (Te) of 15 km and 25 km. Other parameter values as in Table 4 (generic model).

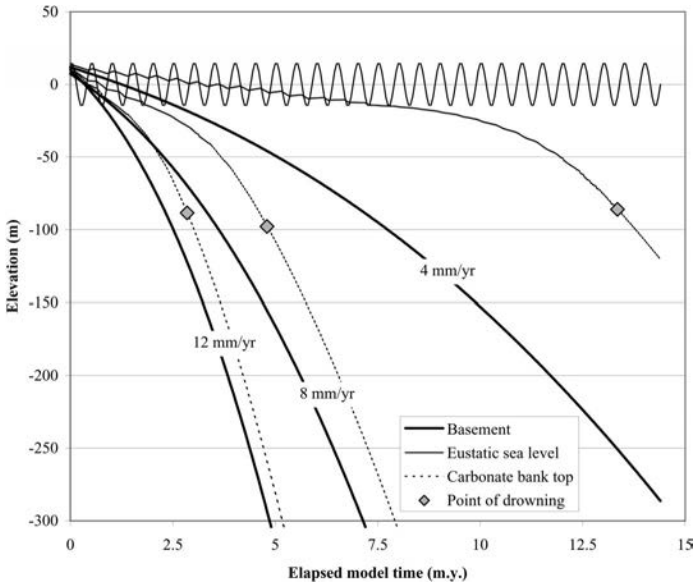

Figure 9. Model results using convergence rates of 4 mm yr^{-1}, 8 mm yr^{-1}, and 12 mm yr^{-1}. Other parameter values as in Table 4 (generic model).

MODEL RESULTS

We first present a standard generic case (Fig. 7) with the parameter values given in Table 4 to indicate the general behavior of the model. We then explore the sensitivity of the model to variations in two tectonic parameters, the flexural rigidity of the plate (Fig. 8) and the convergence rate (Fig. 9), and one environmental parameter, the light-extinction coefficient (Fig. 10). The model is then run with sets of parameter values appropriate for the late Paleocene−middle Eocene of Switzerland and the late Eocene of France (Figs. 11 and 12). In the model output in Figures 7–12, the depth to basement and the depth to the top of the carbonate bank are tracked through model time. The total duration of carbonate deposition before drowning and the total thickness of carbonate can be compared easily with field data (Table 4).

In the generic case (Fig. 7), nummulite bank accumulation begins above a subaerial unconformity at the start of the model run. Early carbonate cycles within an overall retrogradational succession are thin, dominated by shallow-water facies and bounded by surfaces of subaerial emergence that formed during eustatic lowstands. Cycle thicknesses increase upward because of the absence of depositional hiatuses and comprise deeper water facies with no subaerial emergence. Upper cycles become very thin due to the limiting effect of water depth on carbonate accumulation. Eventually the bank is abruptly drowned during a relative sea-level rise at an elapsed model time of ~5 m.y., and then continues to subside into water depths too deep for carbonate accumulation. The carbonate bank attains a maximum thickness of slightly less than 60 m, comprising 10 facies cycles driven by eustatic change.

The effect of flexural rigidity can be illustrated by comparing the two model runs in Figure 8, where all other parameters are the same as in Table 4. The weaker plate increases the rate of tectonic subsidence in the distal foreland basin, causing early drowning of the bank and the preservation of relatively few cycles. When the plate is stronger, the tectonic subsidence rate in the distal part of the basin is smaller, which keeps the bank within the carbonate-producing zone for longer periods of time, allowing more cycles to be preserved. Stratigraphic thicknesses reflect the interplay of bank duration and carbonate accumulation rates. The rapid drowning with the weak plate results in a thinner stratigraphy in these model runs. Cycles show the same pattern of thickening, then rapidly thinning upward through an overall retrogradational package.

The sensitivity of the model to variations in the convergence rate is illustrated in Figure 9. The model was run at convergence rates of 4 mm yr^{-1}, 8 mm yr^{-1}, and 12 mm yr^{-1}, with the standard set of parameter values shown in Table 4. The fast convergence rate causes the carbonate bank to subside rapidly as the flexural wave advances, whereas at slow convergence rates the bank remains in the carbonate-producing zone for a long time. Consequently, bank duration, stratigraphic thickness, and number of cycles decrease with increasing convergence rate. With a fast convergence rate of 12 mm yr^{-1}, the carbonate bank accumulates <20 m of sediment over a period of ~3 m.y., with 5 cycles preserved. This is a plausible explanation for Alpine field data. With

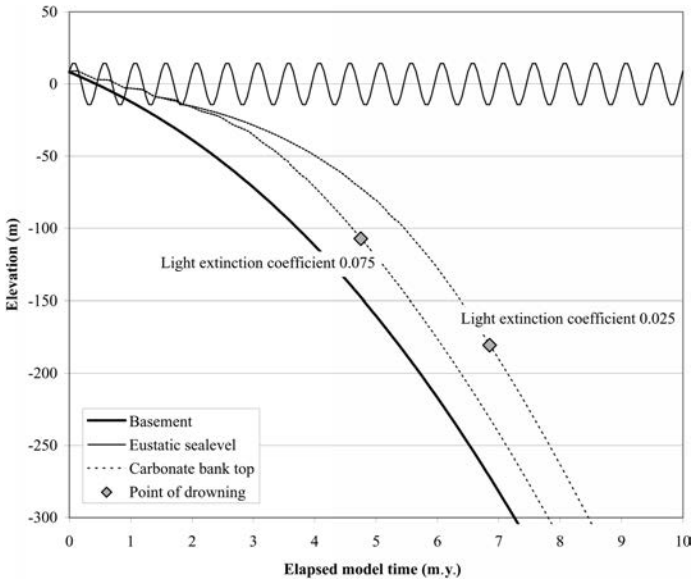

Figure 10. Model results using light-extinction coefficients of 0.025 and 0.075 m^{-1}. Other parameter values as in Table 4 (generic model).

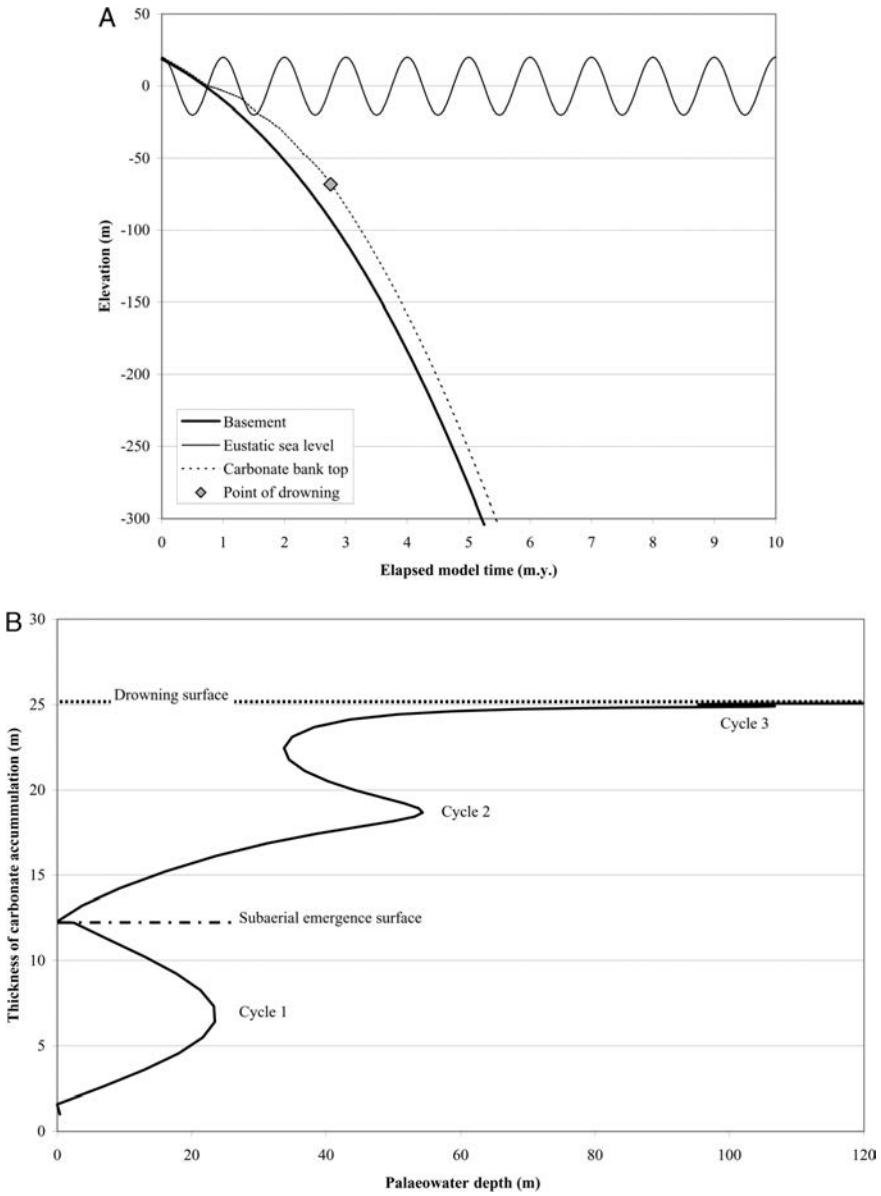

Figure 11. Model output for a set of parameter values (Table 4) applicable to the early-middle Eocene of Switzerland. (A) Conventional output showing bank thickness versus time. (B) Synthetic stratigraphic section showing three eustatically driven cycles below drowning surface.

the moderate convergence rate of 8 mm yr^{-1}, the bank accumulates ~55 m of sediment over a period of 5 m.y., preserving 7 cycles. With the slow convergence rate of 4 mm yr^{-1}, the bank accumulates large thicknesses of carbonate sediment (165 m) because it is easily able to keep up with flexural subsidence. The bank is drowned after 13 m.y. with 26 cycles of 500 k.y. duration preserved. This slow case is not supported by Alpine field data.

Figure 10 shows the sensitivity of the model to variations in the light-extinction coefficient. A threefold variation in light-extinction coefficient has a second-order effect compared to variations in elastic thickness and convergence rate. The higher light-extinction coefficient of 0.075 m^{-1} accentuates the depth dependency of carbonate production, causing carbonate to accumulate more slowly and the bank to drown earlier.

The late Paleocene–middle Eocene Nummulitic Limestone in Switzerland can be approximated best by the parameter values given in Table 4 (Te = 20 km, convergence rate of 12 mm yr^{-1}, and eustatic period of 1 m.y.). The model output (Fig. 11, A and B) shows two well-developed cycles, each >~10 m thick, dominated by shallow-water facies, followed by an extremely thin cycle of deep-water deposits before bank drowning. The entire succession has a duration of ~3 m.y. and total thickness of 25 m. Best estimates from field data (Table 1) suggest 2 to 3 cycles preserved, 20–30 m for carbonate thickness and <6.5 m.y. for the duration of carbonate deposition. This model result therefore satisfies most of the field observations reasonably closely, but we are unable to replicate long periods of carbonate deposition with any reasonable combination of parameter values. Increasing the elastic thickness to 25 km has the unwanted result of increasing carbonate thickness and facies cycles to unjustified values (43 m and 5 cycles).

The late Eocene Nummulitic Limestone of France is best approximated by the parameter values given in Table 4 (Te = 15 km, convergence rate 8 mm yr^{-1}, and eustatic period of 400 k.y.). The model output (Fig. 12, A and B) shows 8 cycles preserved, which initially thicken and deepen upward before thinning and rapidly deepening upward to the drowning surface. Drowning takes place after <~3 m.y., with the preservation of 36 m of stratigraphy. Best estimates from field data (Table 1) suggest as many as 9 cycles comprising 30–40 m carbonate thickness over ~3 m.y. This model result therefore very satisfactorily replicates the field observations.

DISCUSSION AND CONCLUSIONS

Although Crampton and Allen (1995) proposed that the Nummulitic Limestone in eastern Switzerland was deposited in a distal foreland basin above a flexural forebulge unconformity, their emphasis was on the spatial and temporal characteristics of the erosional unconformity and on regional patterns of subcropping and onlapping stratigraphy rather than on the architecture of the Nummulitic Limestone. The numerical model, when independently constrained by choices of parameter values derived from geological and geophysical observations and ecological literature, successfully simulates the essential characteristics of the Nummulitic Limestone in terms of duration of deposition, total thickness, and paleowater depths of the stratigraphic package. Using estimates of cycle periodicity from field studies, the approximate number of cycles within the stratigraphic package is adequately predicted by the model.

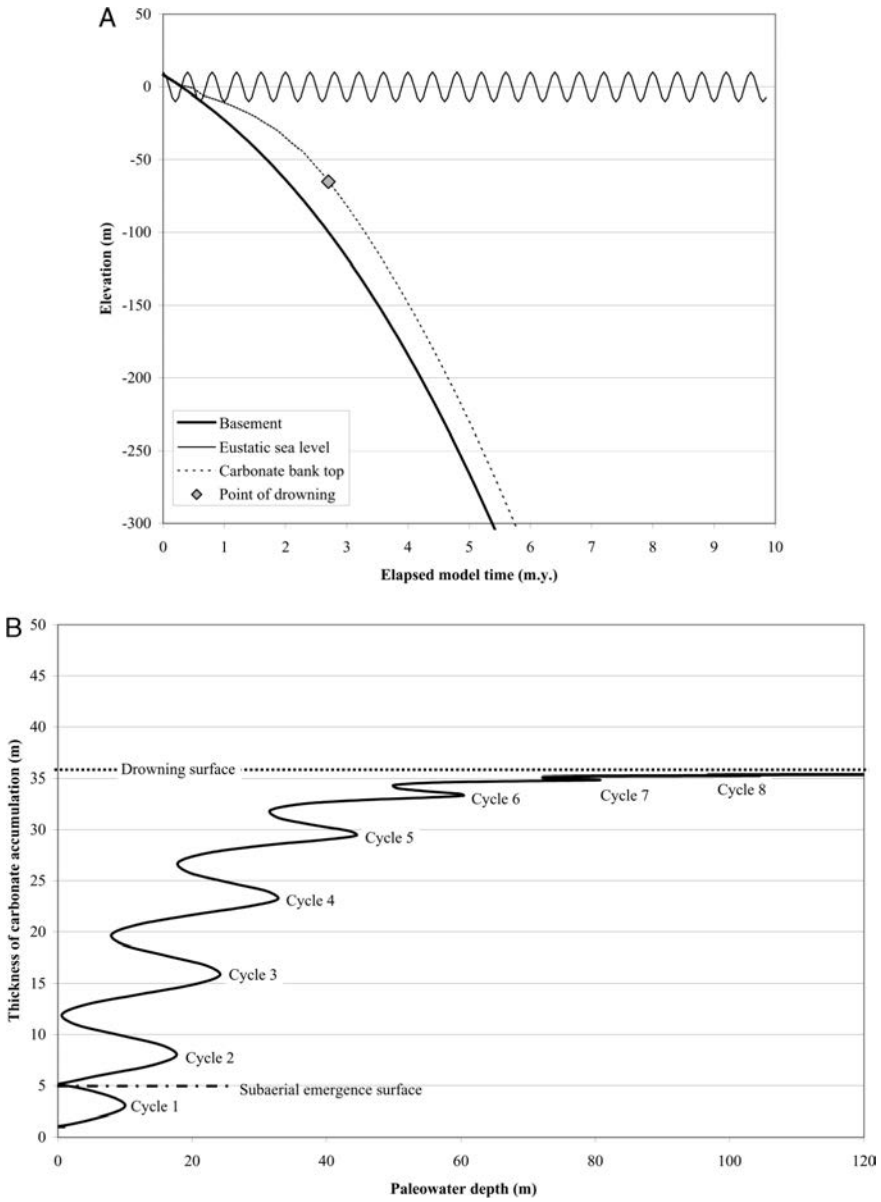

Figure 12. Model output for a set of parameter values applicable to the late Eocene of France. (A) Conventional output of bank thickness versus time. (B) Synthetic stratigraphic section showing eight eustatically driven cycles below drowning surface.

The success of the model in replicating the first-order characteristics of the Nummulitic Limestone in the Alpine foreland during early Tertiary time gives us confidence that the set of parameter values listed in Table 4 is plausible. Although they are clearly not a unique set, there is limited scope for major variation of any of the parameters from their stated values if bank thickness and duration, cycle thicknesses and number, and depositional water depths are all to be replicated simultaneously. Consequently, our results are of significance to the evaluation of geodynamical parameters describing Alpine evolution. In particular, it is highly unlikely that the elastic thickness of the European plate was >20 km and <15 km in Eocene time. A more rigid plate promotes too much and too prolonged carbonate deposition, and too many cycles. A less rigid plate causes almost immediate drowning of the nummulitic bank. Combined with the estimates of Te for 25 Ma, 17 Ma, and the present day given in Table 2, our results appear to rule out any possible secular increase in flexural rigidity of the European plate through the Tertiary. Similarly, it is unlikely that the convergence rate in Eocene time was <8 mm yr^{-1}. A slow convergence rate produces too much carbonate deposition over too prolonged a period of time.

Lateral or secular variations in carbonate productivity caused, for example, by the effects of turbidity on light extinction are likely to have a second-order effect on carbonate accumulation and drowning. Because the one-dimensional numerical model concerns deposition at the distal featheredge of the foreland basin, far-field effects of river plumes derived from the orogen are thought to be minimal. However, it is plausible that the suspended sediments of rivers draining the foreland plate could have a significant effect in compromising or shutting down carbonate productivity in the distal foreland basin. The admixture of siliciclastics in the Bürgen Formation in the Muttsee-Kistenpass region of Glarus, Switzerland (Allen et al., 1991), may be an indication of such a process.

It is unnecessary in the model to begin carbonate deposition in positions beyond the first node in bulge top positions, although this is not excluded as a possibility. To test this possibility will require an a priori eustatic curve for Eocene time. We do not believe that the Haq et al. (1987) model can serve this purpose.

The main conclusions of this study are as follows.

1. Nummulitic Limestone thickness and duration, component cycle thicknesses and number, and stacking patterns vary from place to place in the Alpine foreland. The broad pattern, where the effects of synsedimentary fault activity can be discriminated and accounted for, is of a small number of thin, long-duration cycles preserved in Paleocene to mid-Eocene Nummulitic Limestone in Switzerland, but of a larger number of shorter duration cycles in the late Eocene of France.

2. We have adapted the flexural-eustatic-biological coral platform drowning model of Galewsky (1998) to better suit the foraminiferal buildups of the Alpine periphery in early Tertiary time. Model parameters are constrained as closely as possible from ecological literature and geological and geophysical observations on the Alpine orogen and its peripheral foreland basin. Model runs have been carried out with a maximum carbonate accumulation rate of 0.02 mm yr^{-1}, an extinction coefficient of 0.025−0.075 m^{-1}, a convergence rate of 4−12 mm yr^{-1}, equivalent elastic thicknesses of between 15 and 25 km, and eustatic variations of period from 400 k.y. to 1 m.y. and amplitudes of 10−20 m.

3. The numerical model successfully simulates the first-order characteristics of the Nummulitic Limestone, i.e., its total thickness and duration, number of cycles and cycle thickness, and the overall retrogradational nature of the stratigraphic package. The case for the Nummulitic Limestone as a distal foreland basin carbonate ramp deposited basinward of the first node of the flexed European plate is therefore convincing.

4. The adequacy of the model in simulating the Nummulitic Limestone, and the sensitivity of the model to variations in parameter values, provides an independent corroboration of geodynamic parameters such as convergence rate and particularly flexural rigidity. A convergence rate of 8–12 mm yr^{-1} and an equivalent elastic thickness in Eocene time of between 15 and 20 km appears to be required.

ACKNOWLEDGMENTS

This work builds substantially on the doctoral studies of Sarah Indrelid (née Crampton), Joanne Lihou, Sanjeev Gupta, and Zoë Sayer in the Alps. In addition, we are grateful for the input of Louise Purton (Trinity College) and for the helpful reviews of journal referees Steve Dorobek, David Bice, and Hemmo Bosscher. We also thank Elaine Cullen for her assistance with some of the illustrations.

REFERENCES CITED

Aigner, T., 1983, Facies and origin of nummulitic buildups: An example from the Gisa Pyramids plateau (middle Eocene, Egypt): Neues Jahrbuch Paläontologisches Abhandlungen, v. 166, p. 347–368.

Allen, P.A., Crampton, S.L., and Sinclair, H.D., 1991, The inception and early evolution of the North Alpine foreland basin, Switzerland: Basin Research, v. 3, p. 143–163.

Barbier, R., 1956, L'importance de la tectonique ''anténummulitique'' dans la zone ultradauphinoise au N du Pelvoux: La Chaîne Arvinche: Bulletin de la Socie´té Géologique de la France, v. 6, p. 355–370.

Berggren, W.A., Kent, D.W., Swisher, C.C., and Aubrey, M.-P., 1995, A revised Cenozoic geochronology and chronostratigraphy, *in* Berggren, W.A., et al., eds., Geochronology, time scales and global stratigraphic correlation: SEPM (Society for Sedimentary Geology) Special Publication 54, p. 129–212.

Bice, D.M., 1991, Computer simulation of carbonate platform and basin systems, *in* Franseen, E.K., et al., eds., Sedimentary modeling: Computer simulations and methods for improved parameter definition: Kansas Geological Survey Bulletin 233, p. 431–447.

Bisig, W., 1957, Blattengratflysch und Sardonaflysch im Sernftal nördlich der Linie Richetlipass-Elm-Ramintal-Grosse Scheibe [Ph.D. thesis]: ETH-Zürich, Switzerland.

Bodelle, J., 1971, Les formations nummulitique de l'arc de Castellane: Nice, Bureau de Récherches Géologiques et Minières, v. 1, 581 p.

Bosscher, J., and Schlager, W., 1992, Computer simulation of reef growth: Sedimentology, v. 39, p. 503–512.

Boussac, J., 1912, Etudes stratigraphiques sur le Nummulitique Alpin: Mémoir de Carte Géologique de France, 662 p.

Brasier, M.D., 1980, Microfossils: London, Allen and Unwin, 193 p.

Breitschmid, A., 1978, Sedimentologische Untersuchungen in der eocänen Hoghgant-Serie im Helvetikum nördlich von Interlaken: Eclogae Geologicae Helvetiae, v. 71, p. 143–157.

Burkhard, M., and Sommaruga, A., 1998, Evolution of the western Swiss Molasse basin: Structural relations within the Alps and the Jura belt, *in* Mascle, A., et al., eds., Cenozoic foreland basins of Western Europe: Geological Society [London] Special Publication 134, p. 279–298.

Butler, R.W.H., 1989, The geology of crustal shortening in the western Alps, *in* Şengör, A.M.C, ed., Tectonic evolution of the Tethyan region: Dordrecht, Netherlands, Kluwer Academic Publishers, p. 43–76.

Campredon, R., 1977, Les formations paléogènes des Alpes Maritimes Franco-Italiennes: Mémoires de la Société Géologique de France, v. 9, 199 p.

Chaplet, M., 1989, Etude géologique du massif subalpin du Bornes (Haute Savoie) [Ph.D. thesis]: Chambéry, France, Travaux du Departement des Sciences de la Terre, Université de Savoie, v. 11, 218 p.

Crampton, S.L., 1992, Inception of the Alpine foreland basin: Basal unconformity and Nummulitic Limestones [Ph.D. thesis]: Oxford, University of Oxford, 222 p.

Crampton, S.L., and Allen, P.A., 1995, Recognition of flexural forebulge unconformities associated with early stage foreland basin development: Example from the North Alpine foreland basin: American Association of Petroleum Geologists Bulletin, v. 79, p. 1495–1514.

Debrand-Passard, S., 1984, Synthèse Géologique du Sud-Est de la France. Volume 1: Stratigraphie et Paléogeographie: Mémoires du Bureau de Récherches Géologiques et Minières, v. 125, 615 p.

DeCelles, P.G., and Giles, K.A., 1996, Foreland basin systems: Basin Research, v. 8, p. 105–125.

Deharveng, L., Perriaux, J., and Ravenne, C., 1987, Sédimentologie du flysch des Aiguilles d'Arves (Alpes Francaises): Mémoires de Géologie Alpine, v. 13, p. 329–341.

Demicco, R.V., 1998, CYCOPATH 2D—A two-dimensional forward model of cyclic sedimentation on carbonate platforms: Computers and Geosciences, v. 24, p. 405–423.

Dewey, J.F., Helman, M.L., Turco, E., Hutton, D.H.W., and Knott, S.D., 1989, Kinematics of the western Mediterranean, *in* Coward, M.P., et al., eds., Alpine tectonics: Geological Society [London] Special Publication 45, p. 265–183.

Dorobek, S.L., 1995, Synorogenic carbonate platforms and reefs in foreland basins: Controls on stratigraphic evolution and platform/reef morphology, *in* Dorobek, S.L., and Ross, G.M., eds., Stratigraphic evolution of foreland basins: SEPM (Society for Sedimentary Geology) Special Publication 52, p. 127–147.

Dorobek, S.L., Reid, S.K., and Elrick, M., 1991, Foreland response to episodic Antler convergence events, Devonian-Mississippian stratigraphy of Montana and Idaho; effects of horizontal and vertical loads, *in* Cooper, J.D., and Stevens, C.H., eds., Paleozoic paleogeography of the western United States—II: SEPM (Society for Sedimentary Geology) Special Publication 67, p. 487–508.

Elliott, T., Apps, G., Davies, H., Evans, M., Ghibaudo, G., and Graham, R.H., 1985, A structural and sedimentological traverse through the Tertiary foreland basin of the external Alps of south-east France, *in* Allen, P.A., et al., eds., Field excursion guidebook, International Association of Sedimentologists Symposium on Foreland Basins: Fribourg, Switzerland, International Association od Sedimentologists, p. 39–73.

Elrick, M., and Read, J.F., 1991, Cyclic ramp-to-basin carbonate deposits, Lower Mississippian, Wyoming and Montana: A combined field and computer modelling study: Journal Sedimentary Petrology, v. 61, p. 1194–1224.

Ford, M., 1996, Kinematics and geometry of early Alpine, basement-involved folds, SW Pelvoux Massif, SE France: Eclogae Geologicae Helvetiae, v. 89, p. 269–295.

Froitzheim, N., Schmid, S.M., and Frey, M., 1996, Mesozoic paleogeography and the timing of eclogite facies metamorphism in the Alps: A working hypothesis: Eclogae Geologicae Helvetiae, v. 89, p. 81–110.

Galewsky, J., 1998, The dynamics of foreland basin carbonate platforms: Tectonic and eustatic controls: Basin Research, v. 10, p. 409–416.

Gildner, R.F., and Cisne, J.L., 1990, Quantitative modeling of carbonate stratigraphy and water-depth history using depth-dependent sediment accumulation function, *in* Cross, T.A., ed., Quantitative dynamic stratigraphy: Englewood Cliffs, New Jersey, Prentice-Hall, p. 417–432.

Goguel, J., 1936, Déscription tectonique de la bordure des Alpes de la Bleaune du Var: Mémoires de la Service de la Carte Géologique de France, 360 p.

Goldhammer, R.K., Dunn, P.A., and Hardie, L.A., 1987, High-frequency glacio-eustatic sea-level oscillations with Milankovitch characteristics recorded in Middle Triassic platform carbonates in northern Italy: American Journal of Science, v. 287, p. 853–892.

Guellec, S., Mugnier, J.-L., Tardy, M., and Roure, F., 1990, Neogene evolution of the western Alpine foreland in the light of ECORS data and balanced cross-sections: Mémoires de la Société Géologique de France, v. 156, p. 165–184.

Gupta, S., 1994, Early development of the south-west Alpine foreland basin: Controls on sedimentation and stratigraphy in the Champsaur region, south-east France [Ph.D. thesis]: Oxford, University of Oxford, 243 p.

Gupta, S., 1997, Tectonic control on paleovalley incision at the distal margin of the early Tertiary Alpine foreland basin, southeastern France: Journal of Sedimentary Research, v. 67, p. 1030–1043.

Gupta, S., and Allen, P.A., 1999, Fossil shore platforms and drowned gravel beaches: Evidence for high frequency sea-level fluctuations in the distal Alpine foreland basin: Journal of Sedimentary Research, v. 69, p. 394–413.

Gupta, S., and Allen, P.A., 2000, Intraforeland structural palaeotopography during early foreland basin development: Geological Society of America Bulletin, v. 112, p. 515–530.

Hallock, P., 1981, Production of carbonate sediments by selected large benthic foraminifera on two Pacific coral reefs: Journal of Sedimentary Petrology, v. 51, p. 467–474.

Hallock, P., 1985, Why are larger foraminifera large?: Paleobiology, v. 11, p., 195–208.

Hallock, P., Forward, L.B., and Hansen, H.J., 1986, Influence of environment on the test shape of Amphistegina: Journal of Foraminiferal Research, v. 16, p. 224–231.

Handford, C.R., 1993, Sequence stratigraphy of a Mississippian carbonate ramp, north Arkansas and southwestern Missouri. Field guidebook, American Association Petroleum Geologists Annual Convention: Tulsa, Oklahoma, American Association of Petroleum Geologists,13 p.

Haq, B.U., Hardenbol, J., and Vail, P.R., 1987, Chronology of fluctuating sea levels since the Triassic: Science, v. 235, p. 1153–1165.

Hardy, S., Duncan, C., Masek, J., and Brown, D., 1998, Minimum work, fault activity and the growth of critical wedges in fold and thrust belts: Basin Research, v. 10, p. 365–373.

Heim, A., 1909, Über die Stratigraphie der autocthonen Kreide und des Eocäns am Kistenpass, verglichen mit der Facies der helvetischen Decken: Zürich, ETH.

Herb, R., 1988, Eocaene palägeographie und paläotektonic des Helvetikums: Eclogae Geologicae Helvetiae, v. 81, p. 611–657.

Homewood, P., Allen, P.A., and Williams, G.D., 1986, Dynamics of the Molasse basin in western Switzerland, *in* Allen, P.A., and Homewood, P., eds., Foreland basins: International Association of Sedimentologists Special Publication 8, p. 119–217.

Jacobi, R.D., 1981, Peripheral bulge—A causal mechanism for the Lower/Middle Ordovician unconformity along the western margins of the northern Appalachians: Earth and Planetary Science Letters, v. 56, p. 245–251.

Johnson, D.D., and Beaumont, C., 1995, Preliminary results

from a planform kinematic model of orogen evolution, surface processes and the development of clastic foreland basin stratigraphy, *in* Dorobek, S.L., and Ross, G.M., eds., Stratigraphic evolution of foreland basins: Society of Economic Paleontologists and Mineralogists Special Publication 52, p. 3–24.

Jordan, T.E., 1981, Thrust loads and foreland basin evolution, Cretaceous, western United States: American Association of Petroleum Geologists Bulletin, v. 65, p. 2506–2520.

Karner, G.D., and Watts, A.B., 1983, Gravity anomalies and flexure of the lithosphere at mountain ranges: Journal of Geophysical Research, v. 88B, p. 10449–10477.

Kominz, M.A., Miller, K.G., and Browning, J.V., 1998, Long-term and short-term global Cenozoic sea-level estimates: Geology, v. 26, p. 311–314.

Lateltin, O., 1988, Les dépots turbiditiques Oligocènes d'avant pays entre Annecy (Haute Savoie) et la Sanetsch (Suisse) [Ph.D. thesis]: Fribourg, Switzerland, University of Fribourg, 127 p.

Lateltin, O., and Müller, D., 1987, Evolution paléogéographique du bassin des Grès de Taveyannaz dans les Aravis (Haute Savoie) à la fin du Paléogène: Eclogae Geologicae Helvetiae, v. 80, p. 127–140.

Lemoine, M., 1972, Rhythme et modalité des plissements superposé dans les chaînes subalpins méridionales des Alpes occidentales Francaises: Geologisches Rundschau, v. 61, p. 975–1010.

Leupold, W., 1966, Lexique stratigraphique international, Alpes suisses et Tessin méridional: Congrès Géologique International, Commission de Stratigraphie, Centre Nationale de Récherches Scientifiques.

Lickorish, W.H., and Ford, M., 1998, Sequential restoration of the external Alpine Digne thrust system, SE France, constrained by kinematic data and synorogenic sediments, *in* Mascle, A., et al., eds., Cenozoic foreland basins of Western Europe: Geological Society [London] Special Publication 134, p. 189–211.

Lihou, J.C., 1995, A new look at the Blattengrat unit of eastern Switzerland: Early Tertiary foreland basin sediments from the South Helvetic realm: Eclogae Geologicae Helvetiae, v. 88, p. 91–114.

Lihou, J.C., and Allen, P.A., 1996, Geometry of the underfilled North Alpine foreland basin, Switzerland, and the importance of inherited rift margin structures: Basin Research, v. 8, p. 425–442.

Lyon-Caen, H., and Molnar, P., 1989, Constraints on the deep structure and dynamic processes beneath the Alps and adjacent regions from an analysis of gravity anomalies: Geophysical Journal International, v. 99, p., 19–32.

Macario, A., Malinverno, A., and Haxby, W.F., 1995, On the robustness of elastic thickness estimates obtained using the coherence method: Journal of Geophysical Research, v. 100, p. 15163–15172.

Martini, J., 1968, Études de l'Eocène inférieure et moyen des Châines subalpines Savoyardes, Archives des Sciences, v. 21, p. 35–70.

Moore, P.F., 1988, Devonian geohistory of the western interior of Canada, *in* McMillan, N.J., et al., eds., Devonian of the world: Volume 1: Regional syntheses: Canadian Society of Petroleum Geologists Memoir 14, p. 67–83.

Mougin-Grosso, F., and Pairis, J.-L., 1973, Remarques sur la sédimentation tertiare dans la partie est de la structure d'Annot (Alpes des Haute Provence): Annales du Centre Université de Savoie, v. 1, p. 99–118.

Mugnier, J.-L., Guellec, S., Ménard, G., Roure, F., Tardy, M., and Vialon, P., 1990, A crustal scale balanced cross-section through the external Alps as deduced from the ECORS profile: Mémoires de la Société Géologique de France, v. 156, p. 203–216.

Okaya, N., Cloetingh, S., and Müller, S., 1996a, A lithospheric cross-section through the Swiss Alps, II, Constraints on the mechanical structure of a continent-continent collision zone: Geophysical Journal International, v. 127, p. 399–414.

Okaya, N., Freeman, R., Kissling, E., and Müller, S., 1996b, A lithospheric cross-section through the Swiss Alps, I, Thermokinematic modelling of the Neoalpine orogeny: Geophysical Journal International, v. 125, p. 504–518.

Pairis, B., and Pairis, J.-L., 1975, Précisions nouvelles sur la tertiare du Massif de Platé (Haute Savoie): Géologie Alpine, v. 51, p. 83–127.

Pairis, J.-L., 1988, Paléogène Marin et Structuration des Alpes Occidentales Francaises (Domaine Externe et Confins Sub-Occidentaux de Subbrianconnais) [Ph.D. thesis]: Grenoble, Université Joseph Fourier.

Pfiffner, O.A., 1986, Evolution of the north Alpine foreland basin in the central Alps, *in* Allen, P.A., and Homewood, P., eds., Foreland basins: International Association of Sedimentologists Special Publication 8, p. 219–228.

Pigram, C.J., Davies, P.K., Feary, D.A., and Symonds, P.A., 1989, Tectonic controls on carbonate platform evolution in southern Papua New Guinea: Passive margin to foreland basin: Geology, v. 17, p., 199–202.

Racey, A., 1990, Nummulitid biostratigraphy and Palaeogene palaeoenvironments of the Sultanate of Oman [Ph.D. thesis]: London, University of London, 510 p.

Read, J.F., 1980, Carbonate ramp to basin transitions and foreland basin evolution, Middle Ordovician, Virginia Appalachians: American Association of Petroleum Geologists Bulletin, v. 64, p. 1575–1612.

Reiss, Z., and Hottinger, L., 1984, The Gulf of Aqaba; Ecological micropalaeontology: Berlin, Springer-Verlag, 354 p.

Ross, C.A., and Ross, J.R.P., 1985, Paleozoic tectonics and sedimentation in west Texas, southern New Mexico and southern Arizona, *in* Dickerson, P.W., and Muehlberger, W.R., eds., Structure and tectonics of Trans-Pecos Texas: West Texas Geological Society Publication 85–81, p. 221–230.

Röttger, R., 1976, Ecologic observations of *Heterostegina depressa* (Foraminifera: Nummulitidae) in the laboratory and in its natural habitat: Maritime Sediments, v. 1, p. 75–80.

Royden, L.H., 1993, The tectonic expression of slab pull at continental convergent boundaries: Tectonics, v. 12, p. 303–325.

Rüeffli, W.H., 1959, Stratigraphie und Tektonik des eingeschlossenen Glarner Flysches im Weisstannental (St. Galler Oberland) [Ph.D. thesis]: Zürich, Switzerland, ETH-Zürich.

Ruppel, S.C., and Walker, K.R., 1984, Petrology and depositional history of a Middle Ordovician carbonate platform: Chickamauga Group, northeastern Tennessee: Geological Society of America Bulletin, v. 95, p. 568–583.

Sadler, P.M., 1991, Sediment accumulation rates and the completeness of stratigraphic sections: Journal of Geology, v. 89, p. 569–584.

Sandberg, C.A., Poole, F.G., and Johnson, J.G., 1988, Upper Devonian of western United States, *in* McMillan, N.J., et al., eds., Devonian of the world: Volume 1: Regional syntheses: Canadian Society of Petroleum Geologists Memoir 14, p. 183–220.

Sayer, Z.R., 1995, The Nummulitique: Carbonate deposition in a foreland basin setting; Eocene, French Alps [Ph.D. thesis]: Durham, University of Durham, UK, 337 p.

Schlager, W., 1999, Scaling of sedimentation rates and drowning of reefs and carbonate platforms: Geology, v. 27, p. 183–186.

Schlunegger, F., Matter, A., Burbank, D.W., and Klaper, E.M., 1997a, Magnetostratigraphic constraints on relationships between evolution of the central Swiss Molasse basin and Alpine orogenic events: Geological Society of America Bulletin, v. 109, p. 225–241.

Schlunegger, F., Jordan, T.E., and Klaper, E.M., 1997b, Controls of erosional denudation in the orogen on foreland basin evolution: The Oligocene central Swiss Molasse basin as an example: Tectonics, v. 16, p. 823–840.

Schlunegger, F., Slingerland, R., and Matter, A., 1998, Crustal thickening and crustal extension as controls on the evolution of the drainage network of the central Swiss Alps between 30 Ma and the present: Constraints from the stratigraphy of the North Alpine foreland basin and the structural evolution of the Alps: Basin Research, v. 10, p., 197–212.

Schmid, S.M., Pfiffner, O.A., Froitzheim, N., Schönborn, G., and Kissling, E., 1996, Geophysical-geological transect and tectonic evolution of the Swiss-Italian Alps: Tectonics, v. 15, p. 1036–1064.

Schumacher, J., 1948, Zur Gliederung des marinen Lutétian und basalen Priabonien der Schweizer Alpen: Eclogae Geologicae Helvetiae, v. 41, p. 79–88.

Siddans, A.W.B., 1979, Arcuate fold and thrust patterns in the subalpine chains of southeast France: Journal of Structural Geology, v. 1, p. 117–126.

Sinclair, H.D., 1996, Plan-view curvature of foreland basins and its implications for the long term strength of the lithosphere underlying the western Alps: Basin Research, v. 8, p. 173–182.

Sinclair, H.D., 1997, Tectonostratigraphic model of underfilled peripheral foreland basins: An Alpine perspective: Geological Society of America Bulletin, v. 109, p. 323–346.

Sinclair, H.D., and Allen, P.A., 1992, Vertical versus horizontal motions in the Alpine orogenic wedge: Stratigraphic response in the foreland basin: Basin Research, v. 4, p. 215–232.

Sinclair, H.D., Coakley, B.C., Allen, P.A., and Watts, A.B., 1991, Simulation of foreland basin stratigraphy using a diffusion model of mountain belt uplift and erosion: An example from the central Alps, Switzerland: Tectonics, v. 10, p. 599–620.

Sinclair, H.D., Sayer, Z.R., and Tucker, M.E., 1998, Carbonate sedimentation during early foreland basin subsidence: The Eocene of the French Alps, *in* Wright, V.P., and Burchette, T., eds., Carbonate ramps: Geological Society [London] Special Publication 149, p. 205–227.

Spencer, R.J., and Demicco, R.V., 1989, Computer models of carbonate platform cycles driven by subsidence and eustasy: Geology, v. 17, p. 165–168.

Stacher, P., 1980, Stratigraphie, Mikrofacies und Mikropaläontologie der Wang Formation: Beitrage Geologisches Karte der Schweiz: Neues Folge 152: Basel, Kommission der Schweizerischen Geologische.

Stäuble, M., and Pfiffner, O.A., 1991, Processing, interpretation and modelling of seismic reflection data in the Molasse basin of eastern Switzerland: Eclogae Geologicae Helvetiae, v. 84, p. 151–175.

Steffen, P., 1981, Zur Stratigraphie und Paläontologie des helvetischen Eozäns in der Wildhorn-Decke des Berner Oberlands [Ph.D. thesis]: Bern, Switzerland, University of Bern.

Stewart, J., and Watts, A.B., 1997, Gravity anomalies and spatial variations of flexural rigidity at mountain ranges: Journal of Geophysical Research, v. 102, p. 5327–5352.

Tankard, A.J., 1986, On the depositional response to thrusting and lithospheric flexure: Examples from the Appalachian and Rocky Mountain basins, *in* Allen, P.A., and Homewood, P., eds., Foreland basins: International Association of Sedimentologists Special Publication 8, p. 369–392.

Trümpy, R., 1980, Geology of Switzerland: A guide book, Part A: Basel, Komission der Schweizerischen Geologische, 104 p.

Villars, F., Müller, P., and Lateltin, O., 1988, Analyse de la structure du Mont Charvin (Haute Savoie) en termes de tectonique synsédimentaire paléogène. Conséquences pour l'interpretation structurale des châines subalpines septrionales: Paris, Academie des Sciences Comptes Rendus, v. 307, p. 1087–1090.

Waibel, A.F., 1990, Sedimentology, petrographic variability and very low grade metamorphism of the Champsaur Sandstone [Ph.D. thesis]: Genève, Switzerland, Université de Genève, 140 p.

Watney, W.L., Wong, J.-C., and French, J.A., Jr., 1991, Computer simulation of Upper Pennsylvanian (Missourian) carbonate-dominated cycles in western Kansas, *in* Franseen, E.K., et al., eds., Sedimentary modeling: Computer simulations and methods for improved parameter definition: Kansas Geological Survey Bulletin, v. 233, p. 415–430.

Wegmann, R., 1961, Zur Geologie der flyschgebeite sudlich

Elm [Ph.D. thesis]: Zürich, Switzerland, ETH-Zürich, 256 p.
Wiedmann, M., 1984, Paléokarst éocène dans l'Autochthone chablaisien (VS et VD): Bulletin Murithienne, v. 102, p. 119–127.
Wiedmann, M., Franzen, J., and Berger, J.-P., 1991, Sur l'age des couches à cérithes ou couches des diablerets de l'Eocène Alpin: Eclogae Geologicae Helvetiae, v. 84, p. 893–919.
Wieland, B., 1976, Petrographie eozäner siderolitischer Getsteine des helvetikums der Schweiz: Ihre Diagenese und schwache Metamorphose [Ph.D. thesis]: Bern, Switzerland, University of Bern.
Wuellner, D.E., Lehtonen, L.R., and James, W.C., 1986, Sedimentary-tectonic development of the Marathon and Val Verde basins, west Texas, USA: A Permo-Carboniferous migrating foredeep, *in* Allen, P.A., and Homewood, P., eds., Foreland basins: International Association of Sedimentologists Special Publication 8, p. 15–39.
Yang, K.-M., and Dorobek, S.L., 1995, The Permian basin of west Texas and New Mexico: Tectonic history of a ''composite'' foreland basin and its effects on stratigraphic development, *in* Dorobek, S.L., and Ross, G.M., eds., Stratigraphic evolution of foreland basins: SEPM (Society for Sedimentary Geology) Special Publication 52, p. 149–174.
Ziegler, P., 1988, Evolution of the Arctic−North Atlantic and the Western Tethys: American Association Petroleum Geologists Memoir 43, 198 p.
Zwahlen, P., 1986, Die Handerthal-störung, eine transversale discontinuität im bau der helvetischen Decken [Ph.D. thesis]: Bern, Switzerland, University of Bern.
Zweigel, J., and Zweigel, P., 1998, Plan-view curvature of foreland basins and its implications for the palaeostrength of the lithosphere underlying the western Alps: Discussion: Basin Research, v. 10, p. 271–278.

MANUSCRIPT RECEIVED BY THE SOCIETY MAY 24, 1999
REVISED MANUSCRIPT RECEIVED JULY 7, 2000
MANUSCRIPT ACCEPTED DECEMBER 21, 2000

Printed in the USA